The fate of nitrogen and sulphur during co-liquefaction of algae and bagasse: Experimental and multi-criterion decision analysis

Farah Obeid [a], Thuy Chu Van [a,b], Bingfeng Guo [d], Nic C. Surawski [c], Ursel Hornung [d], Richard J. Brown [a], Jerome A. Ramirez [a], Skye R. Thomas-Hall [e], Evan Stephens [e], Ben Hankamer [e], Thomas Rainey [a,*]

[a] *Biofuel Engine Research Facility, Queensland University of Technology, 2 George St, Brisbane, Queensland, 4000, Australia*
[b] *Vietnam Maritime University, 484 Lach Tray St, Haiphong City, 180000, Viet Nam*
[c] *University of Technology Sydney, 81 Broadway, Ultimo, NSW, 2007, Australia*
[d] *Institute for Catalysis Research and Technology, Karlsruhe Institute of Technology (KIT), Hermann-von-Helmoltz-Platz 1, 76344, Eggenstein-Leopoldshafen, Germany*
[e] *The University of Queensland, School of Agriculture and Food Sciences, Algae Biotechnology Laboratory, Brisbane, QLD, 4072, Australia*

ARTICLE INFO

Keywords:
Microalgae
Bagasse
Hydrothermal liquefaction (HTL)
Co-liquefaction
Biocrude
Nitrogen (N)
Sulphur (S)
Principal component analysis (PCA)
PROMETHEE and GAIA

ABSTRACT

The removal of nitrogen (N) and sulphur (S) from biocrude oil produced using hydrothermal liquefaction (HTL), is important for the production of high quality renewable fuels. Here the effect of co-liquefaction of bagasse and algae was analysed. Algae (*Chlorella vulgaris* and *Cyanobacteria*) were mixed with bagasse (1:1) subjected to HTL at 250–350 °C for 10–60 min. Higher HTL temperatures had a positive effect in increasing the biocrude yield and slightly reduced N content; S did not show a consistent trend. Most of the nitrogen (~66%) and sulphur (~80%) were recovered in the aqueous phase rather than in the biocrude phase, opening the opportunity to recycle these nutrients for algae cultivation. Co-liquefying bagasse with algae improved the biocrude yield (54 wt%) compared to pure *Cyanobacteria* (47.5 wt%). It also reduced N content from 7 wt% (Cyanobacteria biocrude) to 4.2 wt% (Cyanobacteria: Bagasse) and S from 0.7 wt% to 0.4 wt%. Principal Component Analysis (PCA) analysis identified that biocrude yield is positively correlated with the initial lipid content and anti-correlated with the carbohydrates fraction. Biocrude N content is closely related to the initial amount of proteins in the algae. The Preference Ranking Organization METHod for Enrichment of Evaluations and its descriptive complement Geometrical Analysis for Interactive Aid (PROMETHEE and GAIA) analysis ranked the co-liquefaction of *Chlorella vulgaris* and bagasse (1:1) at 350 °C and 60 min as one of the best overall combination in terms of biocrude yield, N and S content.

1. Introduction

In 2017 the global economy was valued at US$127 trillion (GDP, purchasing power parity) [1], and was powered by an energy sector valued between US$6.35 and US$17.78 trillion (historically 5–14% of the GDP) [2]. Internationally, ~80% of this global energy demand is supplied in the form of fuel while electricity provides ~20% [3]. By 2050 approximately 50% more fuel [4] and 80% CO_2 emissions reductions compared to 2005 [5] will be required. Meeting these targets is essential to maintain economic, social, political, climate and fuel security. While significant advances have been made in renewable electricity generation and electric vehicles, fuels are forecast to remain essential for the foreseeable future power aviation, shipping, long-haul transport, heavy machinery and industrial processes.

The production of renewable fuels requires access to a large renewable energy resource. Plants have evolved to tap into the huge energy resource of the sun (3020 ZJ yr^{-1}; ~5000 our total global energy demand) and to use this energy to produce biomass and molecular oxygen which support our biosphere. Biomass by this means, has gained increasing attention since the early 2000s as a cheap and abundant feedstock for the production of renewable fuels [6]. First generation biofuels used food crops, for the production of renewable fuels (e.g. corn ethanol) but resulted in *food vs. fuel* concerns and did not align well with UN sustainability goals [7]. To address these *food vs. fuel* concerns, second generation biofuels, focused on deriving fuels from food waste and agricultural residue (such as bagasse); but their availability still

* Corresponding author. Queensland University of Technology, 2 George St, Brisbane, QLD, 4001, Australia.
E-mail address: t.rainey@qut.edu.au (T. Rainey).

depends on using arable land and biomass extraction for the production of fuel can also adversely affect carbon cycles. Third generation algal biomass offered additional advantages [8]. Microalgae systems can be located on non-arable expanding global photosynthetic capacity, capture CO_2, use saline and/or waste water for biomass production and enable effective recycling of nutrients (e.g. nitrogen and phosphorous) in contained systems. This reduces eutrophication and reliance on energy-intensive chemical fertilisers. The deployment of these systems on non-arable land can also be considered a much needed, technology to assist reversal of desertification.

Algae provide an attractive biomass; their diversity in composition (i.e. lipids, proteins and carbohydrates) serves as a platform for the production of a wide range of renewable fuels products such as renewable diesel, petrol, aviation and shipping fuels as well as ethanol, methane and hydrogen [8]. Conversion routes commonly used are (i) transesterification, a chemical process which converts the lipid fraction to biodiesel, (ii) thermochemical routes such as pyrolysis (dry process) and liquefaction (wet process) which converts algae to a biocrude oil and (iii) biochemical routes such as fermentation and anaerobic digestion [9]. Hydrothermal liquefaction (HTL), is a process operating at high temperature and pressure in the presence of water, and is emerging as the most suitable biomass to crude oil conversion route from high moisture algae biomass with its complex composition [10]. HTL has been extensively studied using a wide range of algae species [10–12], temperatures (250–375 °C), residence times (5–120 min) [10] and catalyst [13]. Algae biocrude often contains high N (5–10 wt%) and S (0.5–1.5 wt%) levels which is problematic in terms of the thermal stability of the fuel and combustion engine emissions (NO_x and SO_x) [14]. Hydro-treating is a route for upgrading and refining of biocrude to reduce N, S, O and aromatic content [11,12]. While hydro-treating remains an expensive route, N and S content could be reduced through co-liquefaction of algae and lignocellulosic biomass.

N in algae species can be classified as protein-N (PN) and non-protein-N (NPN) [15]. Lourenço et al. [16] studied the distribution of N in different algae species, cultivated in different culture media; the accumulated amino acid-N ranged between 63 and 94 mg/100 mg N and NPN 2–35 mg/100 mg N of total N (TN) in the algae. Several studies have analysed the formation of N-containing compounds in algae biocrude oil through the decomposition and the interactions between proteins, lipids and carbohydrates fractions of algae [17–20]. For example, Shu et al. [19] suggested that the formation of pyrazines from amino acids and reducing sugar could be either governed by Maillard reaction and Strecker degradation or through deamination [19]. Consequently, model compounds for protein and carbohydrates have been investigated using HTL to evaluate the interaction mechanism between these compounds [21–25]. The HTL of model compounds for proteins (lysine) and carbohydrates (lactose and maltose) showed that the biocrude composition from lysine contained less N-heterocycles (~10 area %) than biocrude from lysine and lactose (~50 area% N-heterocycles) [22]. Whereas, Yang et al. [20] showed that polysaccharides-protein liquefaction resulted in N-containing compounds (40 area%) which were less than for the protein biocrude (~ 60 area% N-compounds). While the HTL of model compounds provides an understanding of the reaction pathways, they may not always be representative of the feedstock. For instance, the protein fraction of algae contains more than fifteen amino acids, the formation of which is also influenced by the culture condition [16]. Therefore, it is important to study the liquefaction of algae and non-algal biomass to understand the influence of their interaction on N distribution and whether it could possibly reduce N content in the biocrude.

Hydrothermal co-liquefaction of algae and other feedstock has gained recent attention for high yields and improved properties (i.e. physical and chemical) of the biocrude [26–29]. For example, Gai et al. [26] studied the co-liquefaction of *Chlorella pyrenoidosa* (11.3 wt% N) and rice husks (4.7 wt% N), under subcritical conditions (200–350 °C and 10–90 min). A large number of nitrogenous compounds were identified in algae biocrude such as amides (28.38%) which decreased (<10%) in the algae/rice husk biocrude. Chen et al. [27] co-liquefied swine manure and wastewater algae, studying the feedstock ratios on the biocrude yield and quality. The amount of nitrogen in the biocrude increased from 16.8% to 43.9% with the addition of swine manure suggesting a reaction between protein derivatives of algae and lipid derivatives of the swine manure [27]. Thus, the challenge in co-liquefaction lies in understanding the interaction of the different fractions of the feedstocks involved and its effect on the fate of N and S.

In this study, the effect of operating conditions on biocrude yield of the co-liquefaction of algae-bagasse was investigated and a detailed analysis of the HTL products to trace N and S in the HTL products (biocrude, aqueous phase, solid residue and gas) was provided. Bagasse was used to represent a lignocellulosic biomass due to its key property of low N (0.3 wt%) and S (0.2 wt%) content and it is a key industrial crop. PCA and PROMETHEE and GAIA were used in the present study to investigate correlations between feedstock biochemical composition, HTL process conditions and their degree of influence on HTL product yields (bio-crude, solid residue, aqueous and gaseous phase yields in wt. %), bio-crude elemental characteristics (C, H, N, S, O) and its higher heating value (HHV).

2. Materials and methods

2.1. Materials

Nannochloropsis gaditana (N. gaditana), Chlorella vulgaris and *Cyanobacteria* were the selected microalgae species. *N. gaditana* was purchased from Astaxa GmbH, Germany, *Chlorella vulgaris* was supplied by Roquette Klotz GmbH & Co. Germany and *Cyanobacteria* algae was provided by University of Queensland (UQ). Bagasse was selected as lignocellulosic biomass, provided by Karlsruhe Institute of Technology (KIT) and was sourced from Brazil. The biochemical composition of *chlorella vulgaris* and *N. gaditana* were provided by the suppliers. Dichloromethane (DCM), HPLC grade, was purchased from EMD Millipore Co. The properties of the feedstock are presented in Table 1. The organic content of the biomass was determined by mixing a sample with deionised water, then drying it at 105 °C to determine the dry-weight. Then the sample was heated to 550 °C for 5 h in a muffle furnace. Organic content of the biomass is the difference in weight of the sample at 105 °C and 550 °C.

Table 1
Ultimate and structural analysis of the microalgae species and bagasse.

	Bagasse	*Chlorella vulgaris*	*Cyanobacteria*	*N. Gaditana*
Structural analysis (wt.%				
Cellulose	35.2	–	–	–
Hemicellulose	24.5	–	–	–
Lignin	22.2	–	–	–
Lipid	–	9.3	N.D.	19
Carbohydrates	–	9.2	N.D.	10
Protein	–	52	N.D.	46
Ash	20.9[a]	7	28.9[a]	6
Elemental analysis (wt.%)				
C	46.2	48.5	39.1	46.8
H	6.3	7.1	6.6	7.3
N	0.3	8.4	7.2	7.3
S	0.2	0.6	0.9	0.8
O*	47	35.4	46.2	37.8
HHV (MJ.kg ^{1})†	18.34	20.44	15.81	19.9

* By difference.
† Calculated by Eqn.1; N.D.: not determined.
[a] Determined by TGA at 800 ^{O}C.

2.2. Experimental procedure

2.2.1. HTL experiments

In this study, HTL experiments were carried out in 25 mL autoclaves (Fig. 1). The stainless-steel autoclaves consisted of a cylindrical container and a metal cap, with maximum operating limits of 40 MPa pressure and 400 °C temperature. Solid concentration of 10% in the slurry was selected as it was observed by previous studies [30] that it caused the maximum biocrude yield. For each run, 1.5 g of feedstock was mixed with 13.5 g of deionised water. The feedstock: water (1:9) mixture was then loaded into the autoclave. For co-liquefaction experiments, a mixture of bagasse: algae: water (0.5:0.5:9) was prepared. The autoclave was tightly closed and purged with nitrogen several times to flush out the air from inside the reactor. The autoclave was then filled with 2 MPa nitrogen and closed using a torque wrench. The autoclaves were weighed before and after each step to allow recording of any material loss and identify leakage in the autoclave. The autoclaves were transferred into gas chromatography (GC) oven and heated at a rate of 40 °C/min. Once the desired reaction temperature was reached, the reactor was kept in the oven for the desired residence time (RT). The experiment was terminated by placing the autoclave in an ice bath. The conditions investigated presented in Table 2, were temperature (250 °C, 300 °C and 350 °C), RT (10 min, 35 min and 60 min) and co-liquefaction (Bag: *Cy* and Bag: *Chl*). The lower and upper temperatures were selected based on the thermogravimetric analysis (TGA) of the feedstock which helped determine the decomposition temperatures of the fractions. A total of fifty-four experiments were carried out governing the different combinations of temperature, residence time, feedstock and feedstock mixtures. The average error was calculated from repeated experiments and found to be between 9.5 and 14%. Therefore, a representative error of 12% is shown as an error bar in Fig. 3 and Fig. 4 (see Table 3) (see Table 4).

2.2.2. Product separation and characterisation

The reactor was opened in a sealed container connected to a pipe with a manometer. The system was purged with nitrogen to flush the air out. After opening the autoclave, the pressure in the container was recorded and a gas sample was withdrawn from a sampling container with a septum for analysis using a gas chromatograph. The composition of the gas was measured by manually injecting 100 µL of the gas sample in an Agilent 7890A gas chromatograph with a 2-m Molsieve 5A column in series with a 2-m Porapak Q column connected to a front flame ionization detector (FID) and a black thermal conductivity detector (TCD). Solid residue was filtered from the liquids by vacuum filtration using a Whatman nylon membrane (47 mm, 0.45 µm pore size). In order to wash all the biocrude from the autoclaves, dichloromethane (DCM) was used for rinsing. The solid residues were placed in an oven and dried overnight at 105 °C to determine dry weight. The aqueous phase (AP) was separated from the biocrude oil using a syringe to remove the top phase, and weighed. DCM was evaporated by flushing the biocrude with nitrogen gas. The biocrude and solid residue yield were expressed in wt. % and gas (G) yield was determined by difference.

A characterisation of the aqueous phase was carried out. The total carbon (TC), total inorganic carbon (TIC) and total nitrogen (TN) were measured using a Dimatec® 2000 instrument. Total organic carbon (TOC) was calculated by subtracting TIC from TC. Sugars in the aqueous phase were analysed using Shimadzu HPLC equipped withan Aminex HPX-87H column and UV and refractive index detectors. To study the thermal degradation characteristics of the feedstock, thermogravimetric analysis (TGA) was carried out using a Mettler Toledo DSC 822 system, under N_2 flow with a heating rate of 10 °C/min, from 20 °C to 800 °C. The elemental composition (CHNS) of the feedstock, biocrude and solid residue were measured using a Vario EL III elemental analyser device, and oxygen content was calculated by difference. The elemental composition of the feedstock and biocrude was used in Lloyd-Davenport formula (Eqn. 1) to calculate higher heating value (HHV) [31];

$$HHV\ (MJ.kg^{-1}) \quad 0.35777\ C + \quad 0.91758\ H \quad 0.08451\ O \quad 0.05938\ N + 0.11187\ S \quad (1)$$

C carbon (wt.%), H hydrogen (wt.%), O oxygen (wt.%), N nitrogen (wt.%) and S sulphur.

The N, C and S distribution in the HTL products (biocrude, aqueous phase and solid residue) were calculated based on the elemental analysis of the biocrude and solid residue, and the TN and TC of the aqueous phase and used in Eqn. 2 [18].

$$ND\% \quad \frac{\text{N\% x weight of product}}{\text{N\% x weight of nitrogen in dry feedstock}} * 100$$

$$CD\% \quad \frac{\text{C\% x weight of product}}{\text{C\% x weight of carbon in dry feedstock}} * 100$$

$$SD\% \quad \frac{\text{S\% x weight of product}}{\text{S\% x weight of sulphur in dry feedstock}} * 100$$

ND: nitrogen distribution, CD: carbon distribution, SD: sulphur distribution.

2.3. Principal Component Analysis (PCA)

PCA was used in this study as a quantitative tool to perform dimensionality reduction on a detailed HTL dataset, and to establish a relationship between experimental variables and their observations in the new co-ordinate space obtained by PCA. This useful quantitative tool has also been used in similar previous studies [21,32]. In a detailed explanation that is also described in a previous study [33,34], new variables (i.e. Principal Components (PCs)) are found, which are a linear combination of the existing variables. PCs are found in a way such that they are mutually orthogonal to each other with the direction of the first co-ordinate axis capturing most of the variation in the original dataset *X,* the 2nd most variation and so on for the value of n principle components analysed. The value of PCA is that it compresses a high dimensional space to a low dimensional space, while still capturing most of the variance in the original dataset. The algorithm to perform PCA determines the Singular Value Decomposition (SVD) of *X*. The SVD produces two orthogonal matrices (U and V^T) which come from the left and right singular vectors, as well as a square matrix (D) that contains the singular values, given by:

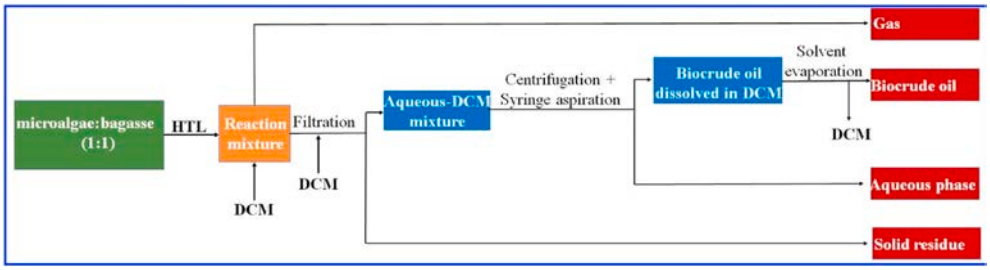

Fig. 1. Experimental setup for Hydrothermal co-liquefaction of algae and bagasse.

Table 2
Experimental conditions tested, T, RT and feedstock combination.

Operating conditions		Feedstock					
Temperature (°C)	RT (min)	Bag	*Chlorella*	*Cyano*	*N. Gaditana*	*Bag: Chl* (1:1)	*Bag: Cy* (1:1)
250	10	x	x	x	x	x	x
	35	x	x	x	x	x	x
	60	x	x	x	x	x	x
300	10	x	x	x	x	x	x
	35	x	x	x	x	x	x
	60	x	x	x	x	x	x
350	10	x	x	x	x	x	x
	35	x	x	x	x	x	x
	60	x	x	x	x	x	x

Table 3
Elemental composition (wt%), molar ratios and HHV (MJ.kg-1) of the biocrude oil from different feedstock at 250, 300 and 350 °C, RT 10 min.

Species	T (°C)	Biocrude									
		C	H	N	S	O*	H/C	O/C	N/C	S/C	HHV†
Bagasse	250	58	6	0.2	0.1	35.7	1.23	0.46	0.003	0.0006	23.24
	300	67.3	6.8	0.3	0.1	25.5	1.20	0.28	0.004	0.0006	28.16
	350	69	7	0.3	0.1	23.6	1.21	0.26	0.004	0.0005	29.11
Chlorella vulgaris	250	65.4	8.8	6.5	0.7	18.6	1.60	0.21	0.085	0.0040	29.59
	300	71	9.4	7.1	0.6	11.9	1.57	0.13	0.086	0.0032	32.67
	350	73.5	9.2	6.6	0.5	10.2	1.49	0.10	0.077	0.0026	33.54
Bag: *Chl*	250	62.3	8.6	6.2	0.4	22.5	1.64	0.27	0.085	0.0024	27.96
	300	69.2	8.1	7.5	0.3	14.9	1.39	0.16	0.093	0.0016	30.52
	350	74.6	8.5	4.8	0.3	11.8	1.35	0.12	0.055	0.0015	33.24
Cyanobacteria	250	52.8	8	7.1	0.7	31.4	1.80	0.45	0.115	0.0050	23.23
	300	70.8	9.3	7.7	0.7	11.5	1.56	0.12	0.093	0.0037	32.51
	350	70.7	8.8	7	0.9	12.6	1.48	0.13	0.085	0.0048	31.99
Bag: *Cy*	250	62.4	8.1	5	0.5	24	1.54	0.29	0.069	0.0030	27.49
	300	65.8	8	7.7	0.4	18.1	1.44	0.21	0.100	0.0023	28.94
	350	64.4	8	4.2	0.4	23	1.48	0.27	0.056	0.0023	28.23

Table 4
Elemental analysis of aqueous sample from different feedstock at 250, 300 and 350 °C, RT 10 min.

Species		Aqueous Elemental Analysis						
	Temp (°C)	TOC	TIC	TC	TNb	Gluc	Fruc	Xyl
Bagasse	250	9501	0	9501	102	289	43	73
	300	8692	0	8692	74	20	0	0
	350	6571	0	6571	61	20	0	0
Chlorella vulgaris	250	17636	1000	17882	6007	20	21.2	20
	300	12514	1509	14023	5522	20	0	0
	350	9196	2533	11729	5579	20	0	0
Bag: *Chl*	250	12407	0	12407	2422	0	14	0
	300	10400	0	10400	2362	20	0	0
	350	6515	193	6708	1938	20	0	0
Cyanobacteria	250	16257	1000	16280	4701	17	11	0
	300	10680	1401	12080	4788	20	0	0
	350	7910	2283	10193	4786	20	20	20
Bag: *Cy*	250	10866	0	10866	1893	0	14	0
	300	9262	0	9262	1718	20	0	0
	350	6735	0	6735	1840	20	0	0

$$X \quad UDV^T. \tag{3}$$

X can be decomposed into loadings (P) and scores (T) matrices by:

$$X \quad (UD)V^T \quad TP^T. \tag{4}$$

T and P both have interpretations that are simple. The loadings matrix shows contributions of the original variables to a particular PC. If a particular variable strongly influences the resulting PC, elements of P will have a higher magnitude. The scores matrix provides co-ordinates of data in the new co-ordinate space found by the PCA. For this study, the RStudio version 1.0.136 using the FactoMineR [35] and Psych [36] packages were utilised. The data were centred and scaled prior to analysis as is the recommended practice for PCA [37].

There are three main forms of graphical output generated from PCA. Firstly, the variables factor map shows the observed experimental variables on a two-dimensional plane composed of the first two PCs. The resulting plot displays the relationship between the measured variables and their corresponding PCs. Secondly, the individuals factor map plots scores for individuals on the first two PCs. Thirdly, the loadings factor map or a full table result including the percentage of variation explained by each PC and its eigenvalue. PCA plots will be a) loadings plots and b) scores plots.

2.4. PROMETHEE and GAIA

PROMETHEE (Preference Ranking Organization Method for Enrichment Evaluations), an object out-ranking method, and GAIA

(Graphical Analysis for Interactive Assistance), a visual data display method, are examples of methods that assist in the making of decisions for multivariate problems; hence the name multi-criteria decision making methods (MCDM). PROMEETHE performs out-ranking by imposing an optimisation criterion on each experimental variable (i.e. to maximise or minimise it) followed by the calculation of preference flows. The application of GAIA is a particularly useful aid because it provides a data display in the form of a Principle Component Analysis bi-plot, and in addition, shows a decision making axis, π, which indicates the quality of the decision. Compared to other methods such as ELECTRE III, SMARTER (Simple Multi-Attribute Rating Technique), PROMETHEE and GAIA preserve as much information as possible, avoiding trade-offs, permit sensitivity analysis, requiring no/minimal interaction by the user, and are readily available in the form of a user-friendly software package. For a more detailed discussion of this method can be seen in previous studies [33,38–40]. In this study PROMETHEE and GAIA was applied to rank HTL conditions and feedstock for HTL bio-crude production by giving equal weight to all criteria. The algorithms for PROMETHEE and GAIA have been described in the Supporting Information.

3. Results and discussions

3.1. Thermal degradation analysis of algae and lignocellulosic feedstock

The biochemical composition of the feedstock influences its decomposition behaviour when undergoing HTL. Thermogravimetric analysis (TGA) was performed using a Mettler toledo DSC 822 under N2-flow with a heating rate of 10 °C·min, from 20 °C to 800 °C. Thermogravimetric analysis (TGA) and differential thermogravimetric analysis (DTG) were used (Fig. 2) in order to understand the decomposition of bagasse, *Chlorella vulgaris, Cyanobacteria* and *N. gaditana*. TGA analysis of bagasse shows two major steps. Step 1 (220–320 °C) corresponds to the degradation of its cellulose and hemicellulose fractions (weight loss of 30.37 wt%) and step 2 (320–400 °C) corresponds to the degradation of the lignin fraction (weight loss of 34.2 wt%). The differential thermogravimetric analysis (DTG) graph of bagasse shows two peaks at 300 °C corresponding to its carbohydrate (i.e. cellulose and hemicellulose) and at 350 °C corresponding to its lignin fractions. *Chlorella vulgaris* TGA showed one major step at 180–340 °C (weight loss of 44.24 wt%) and a minor step at 360–420 °C (weight loss of 10.1 wt%) corresponding to the degradation of its protein and lipid fractions respectively. Its DTG shows two minor peaks at 250 °C and 400 °C corresponding to the degradation of its carbohydrates (9.2 wt%) and lipid (9.3 wt%) respectively, and a major peak at 300 °C corresponding to its protein fraction (52 wt%). *Cyanobacteria* biochemical composition wasn't obtained from the source, however TGA/DTG analysis shows 3-step weight loss: step 1 between 200 and 280 °C (22.8 wt% loss), step 2 between 300 and 380 °C (17.11 wt% weight loss) and step 3 between 390 and 460 °C (16.84 wt% weight loss). These correspond to the degradation of its carbohydrates, protein and lipid fractions respectively. *Cyanobacteria* DTG shows one major peak at 275 °C for carbohydrate and two small peaks at 325 °C (protein) and 400 °C (lipid), we can infer that this cyanobacteria species is carbohydrate-rich. In the case of *N. gaditana*, TGA showed only two major steps, between 180 and 280 °C corresponding to the decomposition of its carbohydrate fraction (22.77 wt% of weight loss) and 310–350 °C (19.85 wt% weight loss) corresponding to the decomposition of its protein fraction. This is in agreement with the literature, identifying the temperature zones for decomposition [41–44]. Campanella et al. [41] identified two zones on the TGA for duckweed, the zone 1 for the protein and carbohydrate fractions which lies between 180 and 350 °C, whereas for the lipid fraction, the zone 2 temperature range is 350–550 °C. Similarly, Babick et al. [42] suggested that decomposition of protein and carbohydrates is at 320 °C but lipid decomposition is initiated at 230 °C. Wang et al. [45] isolated and identified the decomposition temperature of carbohydrates at 275 °C, protein at 310 °C, lipid at 353 °C while *Nanochloropsis* sp. decomposed at 317 °C. Thus protein, carbohydrates and lipid fractions decompose at different temperatures in algae compared to their isolated forms, due to an interaction between them during liquefaction. In addition, the medium of culture for growing algae species plays a role in its cell wall structure, thus influencing its decomposition temperature and the decomposition temperature of the individual fractions [46].

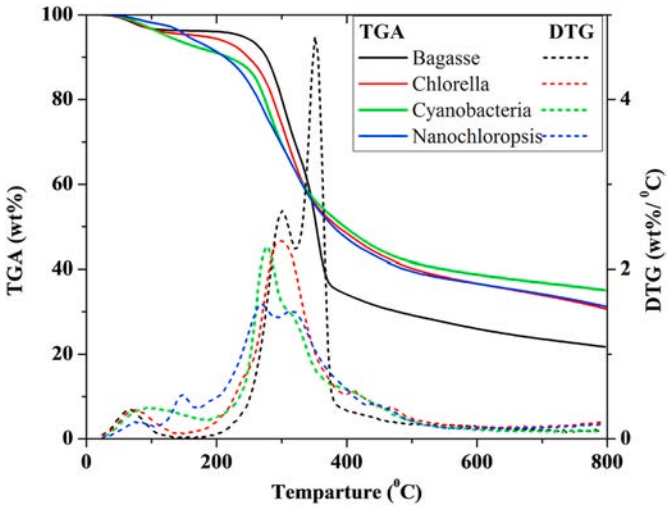

Fig. 2. Thermogravimetric (TG) and differential thermogravimetric (DTG) graphs for algae and bagasse samples.

3.2. Effect of processing conditions and co-liquefaction on biocrude yield

The influence of several processing conditions of HTL, namely temperature and residence time on biocrude oil yield have been extensively investigated [47–50]. Other parameters such as feedstock biochemical composition and slurry concentration have also been explored [46,51]. In most of the HTL studies, it was reported that temperature is the most important parameter affecting the HTL product distribution.

3.2.1. Effect of temperature

In this study, different trends were observed for the biocrude yield with the increase of temperature from 250 °C to 350 °C (Fig. 3). *Cyanobacteria* biocrude yield increased from 33.19 wt% at 250 °C to 34.17 wt% at 300 °C, then the yield reduced to19.02 wt% at 350 °C. In contrast, *Chlorella vulgaris* biocrude yield continued to increase with temperature attaining 43.07 wt% at 350 °C. Whereas, *N. gaditana* biocrude yield decreased from 29.74 wt% at 250 °C to 25.5 wt% at 300 °C then increased to 29.5 wt% at 350 °C. Bagasse biocrude yield showed an increase with increasing temperature from 11.77 wt% at 250 °C to 19.57 wt% at 350 °C. *Cyanobacteria*, *Chlorella vulgaris* and *N. gaditana* behave differently in response to the increase in temperature during hydrothermal liquefaction, this could be attributed mainly to the distinction of their biochemical compositions.

During co-liquefaction of algae-bagasse, it was important to study the effect of temperature on the biocrude yield. The biocrude yield of Bag*: Cy* continued to increase with the increase of temperature from 21.1 wt% at 250 °C to 53.8 wt% at 350 °C. For Bag*: Chl* the biocrude yield increased from 21.7 wt% at 250 °C to 35 wt% at 350 °C. It is worth noting that bagasse biocrude yield was lower than algae biocrude yield in all the studied conditions; however during co-liquefaction the biocrude yield was improved which could be attributed to the Maillard reaction between the protein and the carbohydrate fraction of algae and bagasse, respectively.

3.2.2. Effect of residence time (RT)

The effect of RT on the biocrude yield from the HTL of algae and

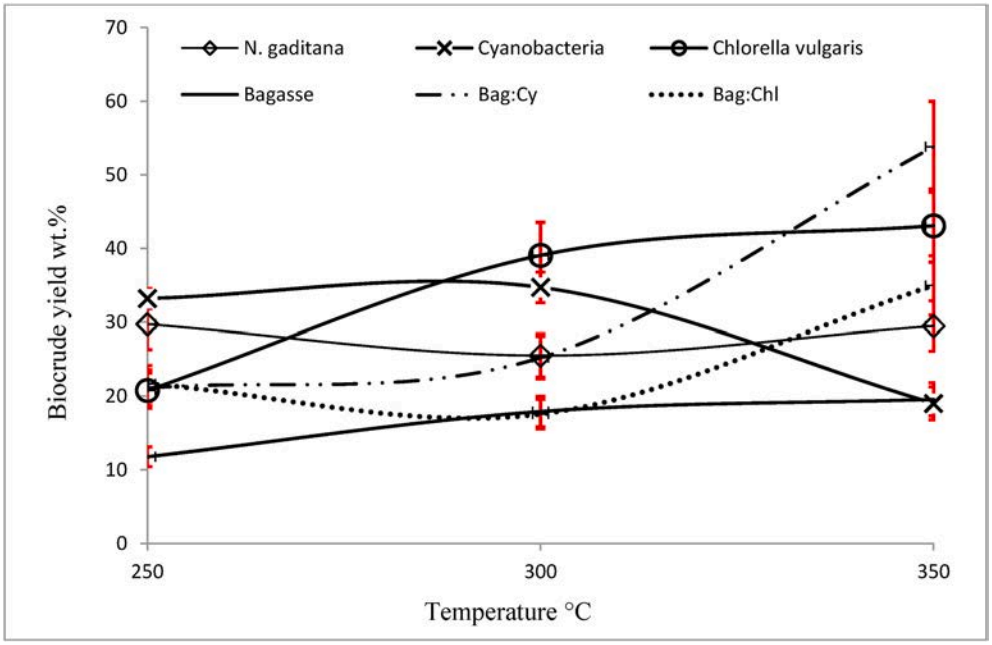

Fig. 3. Effect of temperature on biocrude yield of algae and algae: bagasse at 10 min RT.

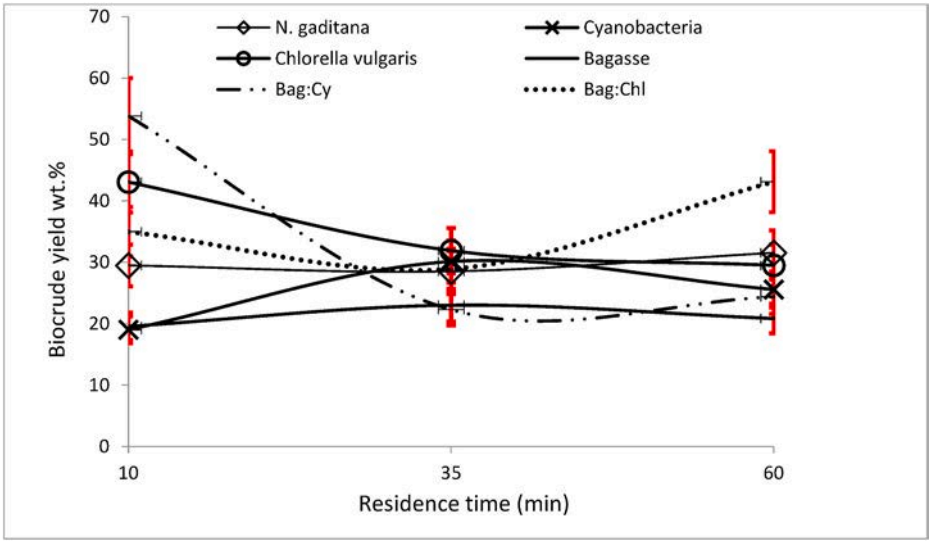

Fig. 4. Effect of residence time on biocrude yield of algae and algae: bagasse at 350 °C.

bagasse and the co-liquefaction of bagasse: algae mixtures are presented in Fig. 4. The biocrude yield of *cyanobacteria* increased with increasing RT 19.02 wt% to 30.12 wt% at 10 and 35 min respectively, then the yield experienced a slight decrease to 25.57 wt% at 60 min. The highest biocrude yield of 43 wt% for *chlorella vulgaris* was achieved at 10 min RT, while longer RT caused considerable decrease in the yield to 32 wt% and 29.5 wt% at 35 and 60 min, respectively. The residence time did not have a significant effect on biocrude yield of N. Gaditana, where the yield was 29.5 wt% at 10 min, experienced a slight decrease to 28.5 wt% at 35 min and then increased to 31.5 wt% at 60 min. Bagasse biocrude experienced a similar trend to *cyanobacteria* with respect to RT. Bagasse biocrude increased from 19.5 wt% at 10 min to 23 wt% at 35 min then slightly decreased to 20.8 wt% at 60 min. The co-liquefaction of Bag: *Cy* at 10 min gave the highest biocrude yield of 53.8 wt%, while longer residence times caused a considerable reduction to the biocrude yield. Whereas for Bag: *Chl*, longer residence times had a positive effect on biocrude yield which increased from 35 wt% at 10 min to 43 wt% at 60 min.

In HTL, temperature and residence time are somewhat linked, as higher temperatures require shorter residence time, which was very clear in the case of *Chlorella vulgaris*. The highest biocrude yield of *Chlorella vulgaris* (43 wt%) was achieved at 350 °C, 10 min. It follows that lower temperatures require longer residence time to produce the highest biocrude yield, as is the case of *Cyanobacteria*, the highest biocrude yield of 47.57 wt% was attained at 300 °C, 60 min.

3.2.3. Effect of biochemical composition of feedstock

The variations of the effect of temperature and residence time on the biocrude yield are related to the biochemical composition of the feedstock processed during HTL and co-liquefaction. It is important to identify the composition of the feedstock to understand its behaviour during processing.

3.2.3.1. Algae composition and degradation behaviour. Algae species are

mainly composed of lipids, proteins and carbohydrates. The growth medium and cultivation conditions affect the composition, such as nitrogen-rich medium promotes the accumulation of the protein. While nitrogen starvation favours the accumulation of the lipids fraction [52].

3.2.3.2. Lipids. The lipid fraction is composed of saturated fatty acids, the dominant lipid is palmitic acid and unsaturated fatty acids such as linolenic acid and oleic acid [53]. These triglycerides hydrolyse under subcritical conditions to become free fatty acids and contribute to the production of biocrude. Thus, high lipid algae species produce more biocrude than low lipid algae [54].

3.2.3.3. Proteins. Amino acids, linked by peptide bonds, are the building blocks of protein. Amino acids contain amine (-NH_2) and carboxyl (-COOH) functional groups. During HTL, proteins undergo deamination to produce ammonia and organic acids and decarboxylation to produce carbonic acid and amines [55]. Dote et al. [17] studied the effect of HTL at 300 °C on 19 different amino acids and observed that their biocrude yield varied between 0.2 and 66.4%. While a number of researchers identified the contribution to biocrude yield to follow the trend of lipid > protein > carbohydrates [51,54], however protein also contributes to the formation of biocrude, especially when algae species lipid content is low [54,56]. In this study, the algae investigated are considered protein-rich; however *N. Gaditana* which had higher lipid content (19 wt %) than *Chlorella vulgaris* (9.3 wt%) gave lower biocrude yield.

3.2.3.4. Carbohydrates. Carbohydrates (cellulose and others) contribute to biocrude production and may convert to benzene, propanoic acid and 4-hydroxyphenethyl alcohol, among others [57]. However carbohydrates may also decompose to water-soluble organics such as glucose and result in lower biocrude yield.

As can be observed in Fig. 5, at lower temperatures, the carbohydrate fraction of *Chlorella vulgaris* decomposed into sugars in the aqueous phase. The biocrude yield may have increased due to reactions unrelated to carbohydrate decomposition.

3.2.3.5. Bagasse composition and degradation behaviour. Bagasse is a lignocellulosic waste which is produced by the extraction of sugar from sugarcane. It is mainly composed of cellulose, hemicellulose and lignin. During HTL at 250 °C, these components decomposed mainly to water-soluble organics. Sugars such as glucose, fructose and xylose at 405 mg/L were identified in the aqueous phase which explains the low biocrude yield of 11.7 wt%. At temperatures beyond 250 °C, these fractions were converted to biocrude, and this resulted in higher yield and lower sugar concentrations in the aqueous products. Fig. 6 presents the effect of temperature, residence time and feedstock (i.e. biochemical composition) on the resultant biocrude yield.

3.3. Effects of feedstocks and operating conditions on HTL bio-crude yield and properties using a multi-criterion decision analysis

PCA was used in the present study to perform dimensionality reduction on a detailed, multi-dimensional HTL dataset and to gain information on the correlations between biomass feedstock biochemical

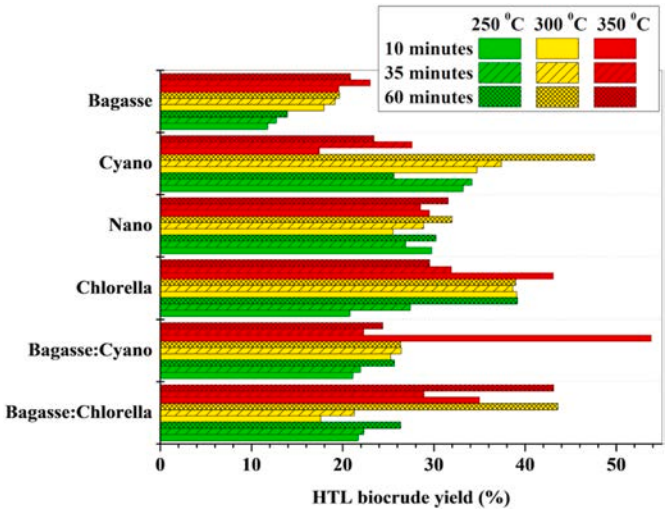

Fig. 6. Effect of temperature, residence time and biochemical composition on the biocrude yield.

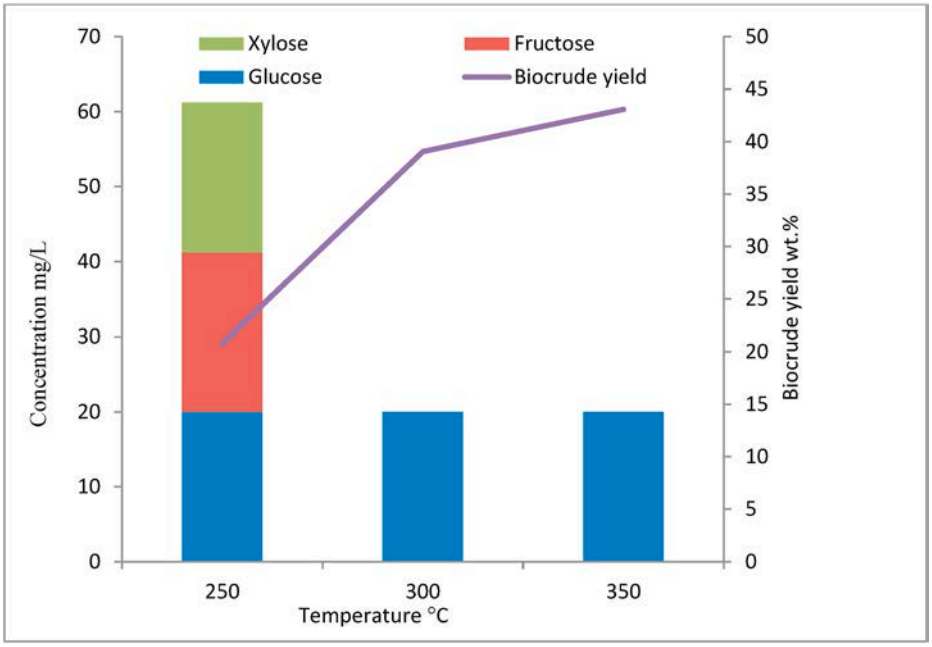

Fig. 5. Concentrations of sugar identified in the aqueous product of Chlorella vulgaris compared to biocrude yield at different temperatures and 10 min residence time.

compositions, HTL product yields and biocrude elemental characteristics. Six PCs of the PCA results cover a total of over 95% of the variance. The percentage of variation explained by each is shown directly on the figure axes. Eigenvalues and percentage of variance explained by each PC can be seen in the Supporting Information. Fig. 7 and Fig. 8 show the variables and individuals factor maps. Further results of this PCA are shown in the Supporting Information. The first two PCs account for around 67% of variance and none of the remaining PCs exceeded 10% of variance. Therefore only the first two PCs are considered in the analysis.

The variables factor map presented in Fig. 7 shows the relationship between the variables. Correlated variables lie close to each other in the graph (±45°), anti-correlated variables lie approximately in opposite directions (135–225°), whilst independent or un-correlated variables lie in a roughly orthogonal direction (45–135°) in the graph. From Fig. 7, it can be seen clearly that ash and carbohydrate were strongly associated with HTL solid residue, AP and GP yields, suggesting that these components from biomass feedstock tended to form solid residue, AP and GP during HTL conversion. Biller et al. [51] stated that carbohydrate is most likely to be broken down to form polar water-soluble organics that do not contribute to HTL biocrude yield. The authors concluded that, based on carbon distributions, carbohydrate not only increased solid formations but also contributed significantly to the gaseous HTL phase. It is believed that biomass feedstock with higher lipid content will be more favourable for HTL, a method of thermochemical conversion, because of the ease in hydrolysis and the high biocrude yield obtained [32]. This is in good agreement with the present study, in which feedstock lipid content is strongly correlated with HTL biocrude yield as can be seen in Fig. 7. Compared to lipid, protein shows a potentially modest correlation with HTL biocrude yield. The conversion efficiency of lipids to HTL biocrude is higher than that for protein. This is consistent with the findings of a previous study that analysed HTL of different model components including lipid, protein and carbohydrate fraction of microalgae [51]. As also can be seen in Fig. 7, protein is closely associated with N content in HTL biocrude. Protein, a polymer of amino acids, decomposes easily and quickly at low temperatures to form carbonic and organic acids, which then re-polymerise to long-chain carbons

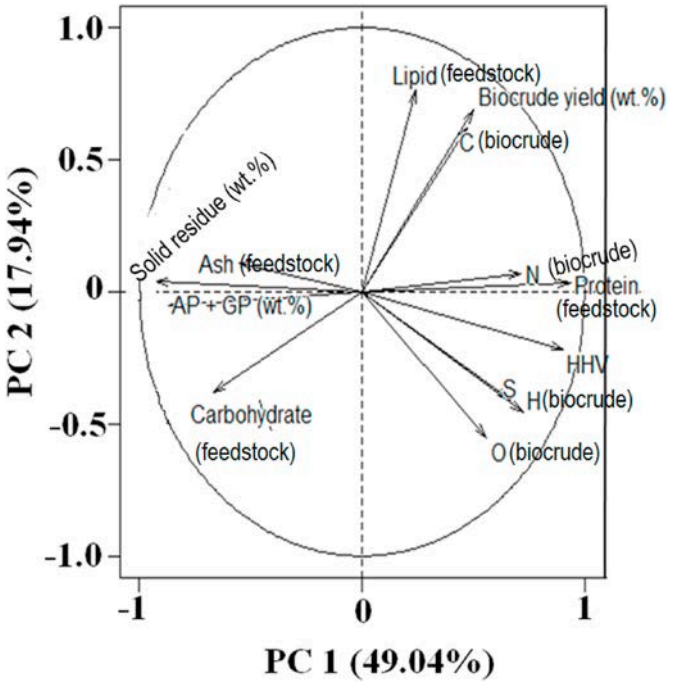

Fig. 7. Variables factor map that is the loading plot from the first two PCs for investigating the correlations between feedstock biochemical compositions, HTL product yields and bio-crude elements.

and N-containing heterocyclic compounds such as pyridine, pyrrole and indole [58]. These compounds are the main source of N in HTL biocrude. Lipids from microalgae are generally in form of triacylglycerol that consists of a glycerol combined with three fatty acids. Under HTL conversion, these fatty acids tended to form long-chain hydrocarbons. As a result, lipids show a significant correlation with C in HTL biocrude as can be found in Fig. 7. The rest of biocrude elemental compositions most likely do not exhibit a well-defined association with biochemical compositions. As can be seen in Fig. 7 that there is a strong correlation between biocrude yield and C content of the biocrude (±45°). However, authors are not able to explain why this has happened. More study is needed to make this clear.

Fig. 8 presents the individual factor map including HTL temperature, retention time, and the biochemical composition of the feedstock. It has been reported in previous studies that HTL conversion temperature has a strong impact on HTL yields and biocrude quality [59,60]. The reaction temperature of 350 °C presented by (red triangles) has a very different profile compared to 250 and 350 °C, as can be seen in Fig. 8a. The data for 350 °C is separated into two main groups which are located at opposite sides of the individual factor map. One group of 350 °C experiments is located to the left of the third quadrant, while others are located between the first and forth quadrant. Combining with Fig. 7, these two groups of 350 °C are strongly associated with HTL biocrude and AP + GP yields, and N content in the biocrude. Jena et al. [50] stated that HTL biocrude yield increase with the increase in reaction temperature, however further increase of the temperature may result in the decline of biocrude yield. This suggests that HTL conversion of biomass is complete. It is also reported that increasing reaction temperature boosted nitrogenated compounds in HTL biocrude [50]. This is in agreement with the finding in this present study. The reaction temperature of 250 °C (green squares) seems to be correlated with solid residue yield. Some recent studies used individual model component of lipid, protein and carbohydrate with HTL and found that the highest HTL biocrude yield from HTL of lipid was observed compared to protein [21, 61]. It is believed that it may be beneficial to use mild conditions (250 °C) to obtain maximum yield of biocrude from the lipid fraction [62]. For HTL reaction temperature of 300 °C, it does not exhibit a clear effect on HTL yields; however, a general trend can be seen here is that high HTL temperature (including 300 and 350 °C) showing a moderate correlation with the higher heating value (HHV) of biocrude. This effect has been reported in previous study [50].

Fig. 8c shows a significant effect of biomass feedstock on HTL biocrude yield and its properties because each type of feedstock behaves similar and is located close together. This strong impact of feedstock may be due to a large variation in the biochemical composition of one compared to others. Biomass feedstock with high lipid and protein are generally favourable for HTL conversion, although N content in HTL biocrude is undesirable [51]. It can be seen clearly that *N. gaditana* and *Chlorella* species are strongly associated with HTL biocrude yield. These species present high lipid content compared to others. In contrast, bagasse with high carbohydrate content gave the lowest biocrude yield. This indicates that protein has a strong impact on N content in the biocrude oil. In particular, *chlorella* and *cyanobacteria* species that have relatively high protein content compared to others are strongly associated with N content of HTL biocrude as can be seen in Fig. 8c.

- PROMETHEE and GAIA

Multi-criteria decision method (MCDM) software PROMETHEE and GAIA was used to make objective selections, rank the most suitable feedstocks for biocrude oil production, and establish what feedstock parameters most affected these rankings. Combining feedstock composition, temperature and time as variables is a total of 63 objects in the matrix, while HTL biocrude, solid residue and AP + GP yields are treated as variables. In general, PROMETHEE is a non-parameter method, which will rank objects (combining feedstock, HTL reaction temperature and

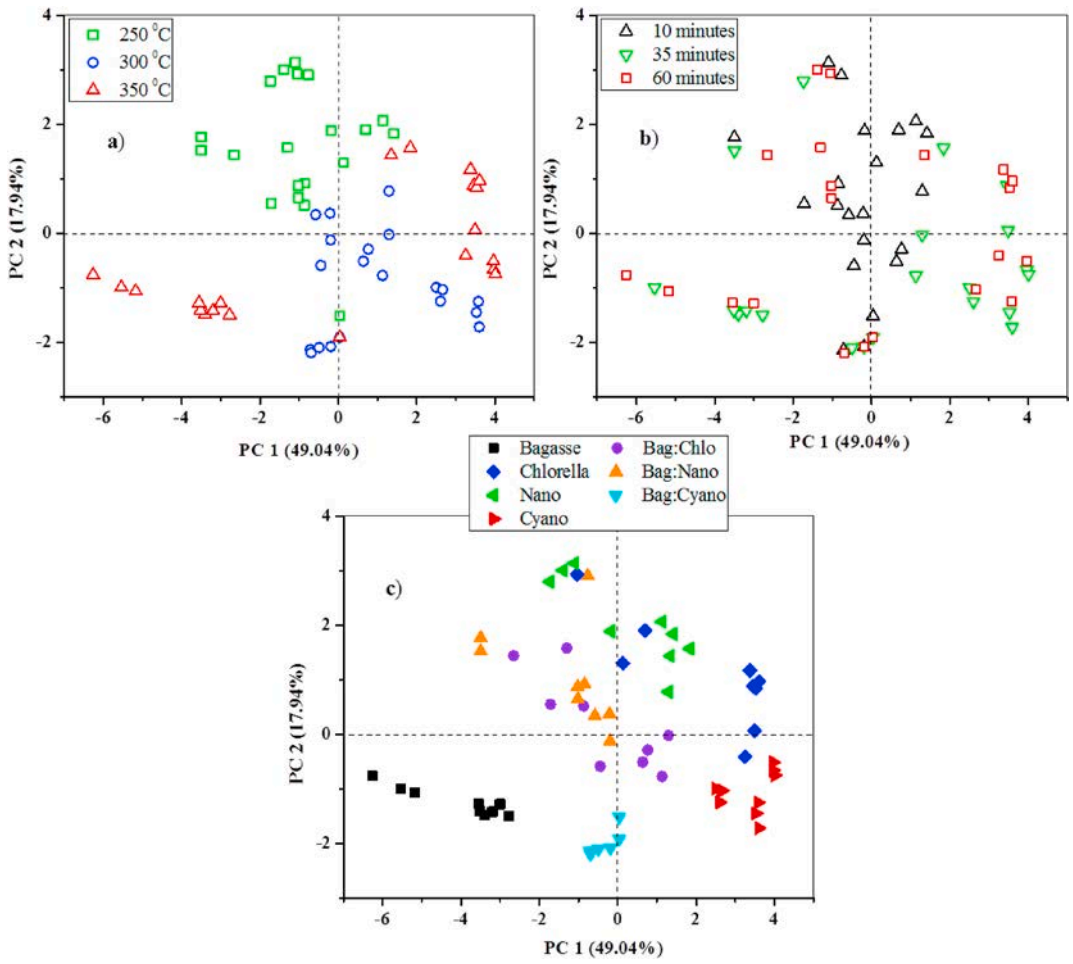

Fig. 8. Individuals factor map (PCA) for a) different HTL temperature conditions; b) different HTL retention time in minutes; c) different biomass feedstock.

time) on the basis of a range of variables (HTL biocrude, solid and AP + GP yields). This method requires that each variable (or criteria) is separately modelled and optimised to either minimise (e.g. lower values are preferred for good HTL conversion) or maximise (e.g. higher values are preferred for good HTL conversion).

In this study, HTL biocrude yield variable was maximised, while HTL solid and AP + GP yield variables were minimised. N and S contents of the biocrude were minimised (to reduce emissions during combustion in an engine) and C and H content were maximised (to improve HHV). The V-shape preference function was used for such criteria. The length of the criteria vectors and their directions indicate the impact of these criteria have on the decision vector (red bold line in Fig. 9a). The decision vector

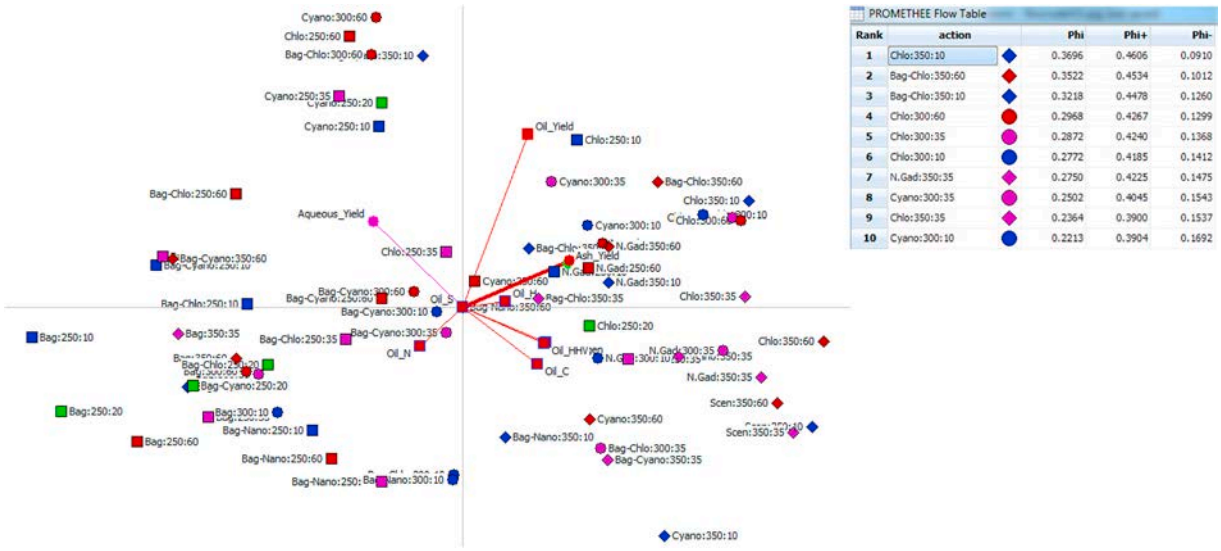

Fig. 9. a) Graphical Analysis for Interactive Assistance (GAIA) plot results and b) corresponding ranking based on the outranking flow.

indicates the most preferable combination of feedstock and HTL conditions, those that locate with the direction of this vector. To aid this, a table of outranking flow, as can be seen in Fig. 9b, shows more details about the ranking and out-ranking (i.e. phi score) for each object. It can be seen clearly that in the top first ten objects, the most suitable feedstock for HTL conversion mainly consists of Bagasse*: Chlorella* (1:1) and *Chlorella vulgaris* in terms of biocrude yield, N and S content. In contrast, variables related to bagasse seem to be not favoured for obtaining high desired HTL biocrude yield.

3.4. The effect of temperature, residence time and co-liquefaction on nitrogen and sulphur content of the biocrude

Algae biocrude's high N content is closely correlated to its high protein fraction, e.g. *Chlorella vulgaris* (protein 52 wt%, N 8.4 wt%) and *Cyanobacteria* (protein 35.2 wt%, N 7.2 wt%). S is also found to play an important role in the structure of the protein fraction of algae, it is also found in sulfolipids and other compounds. S content in algae feedstock is remarkably low (0.6–0.9 wt%). Algae biocrude typically contain 6–10.4 wt% N and 0.5–1.1 wt% S; therefore in most of the investigations carried on algae biocrude, S was overlooked. Although S content is low (~1 wt %) it is still as problematic as N in terms of fuel stability and engine emissions. Current regulations limit S content to 0.01% [63], while algae biocrude contains 100 times more sulphur. It is worth noting that algae biocrude obtained at 250 °C had higher N content than that of the feedstock. For example, the N content of *Cyanobacteria* was 7.2 wt% and *Chlorella vulgaris* was 8.4 wt%, while its resultant biocrude N content was 10.4 wt% and 9.6 wt% respectively. Bagasse, on the other hand, has low N and S content of 0.3 wt% and 0.2 wt% respectively, thus its biocrude had low N and S of 0.2 wt% and 0.1 wt% respectively.

The effect of temperature, RT and co-liquefaction on the content of N and S of the biocrude is presented in Fig. 10. Temperature has a clear influence on N and S content of algae biocrude. The increase in temperature reduced biocrude N content. *Cyanobacteria* biocrude N content was reduced from 10.4 wt% 250 °C to 6.5 wt% at 350 °C. Similarly, *Chlorella* biocrude N content was reduced from 9.6 wt% at 250 °C to 7.2 wt% at 350 °C. S content however didn't show a consistent trend with the increase of temperature; *cyanobacteria* biocrude S content increased with temperature from 0.5 wt% to 1.1 wt% at 250 °C and 350 °C respectively. Whereas that of *chlorella vulgaris* decreased with temperature from 0.7 wt% to 0.5% at 250 °C and 350 °C respectively (Fig. 10a). The inference of residence time influence on biocrude N and S content wasn't as apparent as for temperature (Fig. 10b). However a slight decrease in biocrude N was observed at longer RT, whereas S didn't follow a consistent trend. At 300 °C, *chlorella* biocrude N content was 7.7 wt%, 7.5 wt% and 6.1 wt% at 10, 35 and 60 min respectively, while S content (0.7 wt%) wasn't affected. The biocrude from bagasse: algae mixture had significantly lower N and S contents than for algae biocrude (Fig. 10c). Bag: *Cy* biocrude N and S content were 4.2 wt% and 0.4 wt% respectively, which were considerably lower than that of *Cyanobacteria* biocrude N and S content of 7 wt% and 0.7 wt%, respectively. Similarly, *Chlorella vulgaris* biocrude N and S content were 7.2 wt% and 0.5 wt% whereas that of the Bag: *Chl* biocrude was 4.6 wt% and 0.4 wt%, respectively.

Fig. 11 shows the mass fraction of biocrude and feedstock reported as a ratio. Values less than 1 represent a reduction of N content in biocrude compared to feedstock and values greater than 1, vice versa. Generally single feedstocks show a reduction in N mass fraction during HTL. Almost all blended feedstocks results show an increase in N mass fraction during co-liquefaction. The exact mechanisms for blended feedstocks having increased mass fraction of N during co-liquefaction is not completely clear but could be due to changes in chemical kinetics or low N feedstocks (due to diluting presence of bagasse) increasing to reach an equilibrium value. Bagasse is excluded from the graph as the initial N content (in the denominator) is very low in relation to the experimental error.

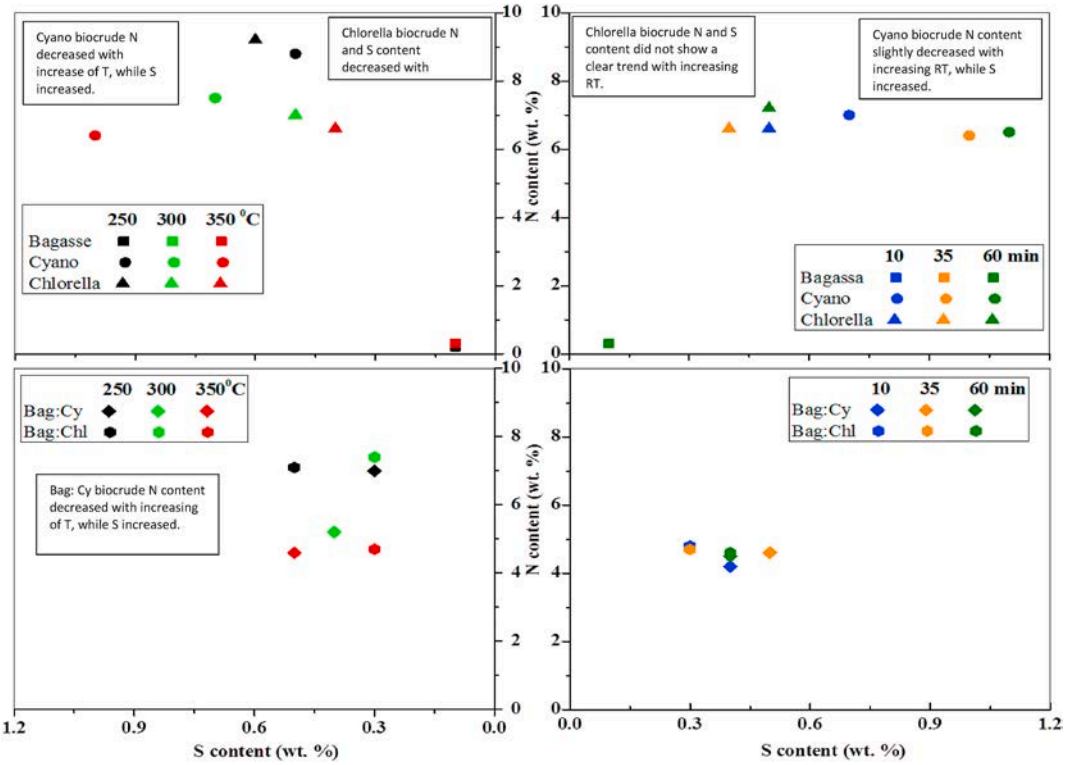

Fig. 10. The effect of a) temperature b) residence time c) co-liquefaction of bagasse: algae on N and S content in the biocrude.

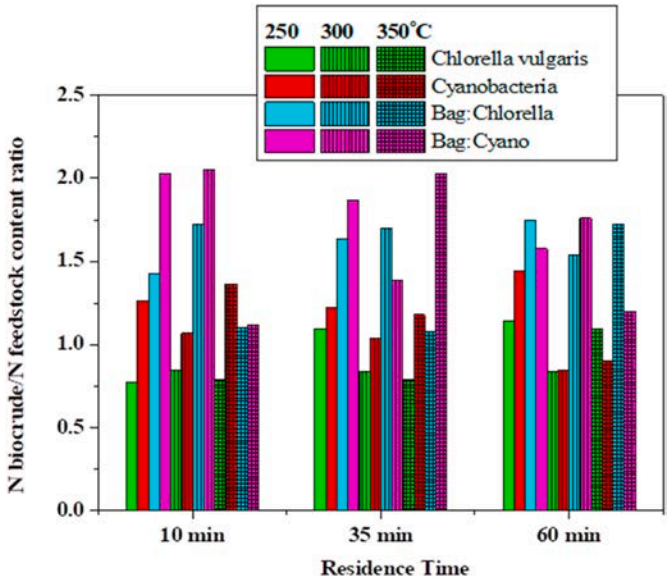

Fig. 11. The change in N content for algae and bagasse co-liquefaction at different operating conditions.

3.5. Analysis of gaseous products from bagasse, cyanobacteria and bagasse-cyanobacteria hydrothermal liquefaction

The analysis of the gaseous products obtained from experiments at 350 °C from *Cyanobacteria*, bagasse and Bag: *Cy* showed the presence of CO_2, N_2, CH_4 and traces of higher hydrocarbons (C_2–C_5), CO_2 being the dominant product (39.5–56.5 vol%) shown in Fig. 12. N_2 (38–51 vol%) was found in in the gaseous products of *Cyanobacteria*, bagasse and Bag: *Cy*. Jena et al. [50] suggested that the presence of N_2 (70–92%), in the gaseous product could be a result of running HTL experiments under a nitrogen atmosphere.

3.6. The effect of temperature on nitrogen, carbon and sulphur distribution and the effect of co-liquefaction on their migration

The N, C and S distribution in the HTL products are shown in Fig. 13. C and N content in the feedstock and their products were all measured individually and it can be seen that the balance is more fully accounted for N than C. This is most likely due to C escaping in the gaseous phase as CO_2, CH_4 and higher hydrocarbons (see Fig. 12). The closure for N is better than that for C due to less gas phase losses.

For *Cyanobacteria* and *Chlorella vulgaris* the majority of nitrogen was found in the aqueous phase (~66%). Increasing of temperatures led to the migration of nitrogen from the biocrude to the aqueous phase. For instance, N retained in the *Cyanobacteria* biocrude at 250 °C was 41.7% which reduced to 24.5% at 350 °C, while the N retained in the aqueous phase increased from 47% to 62.5% respectively. Bagasse N was retained mainly in the solid residue (55–65%). The increase of temperature from 250 to 350 °C led to more N recovered in the biocrude (8–23%).

During co-liquefaction of bagasse and algae, slightly more nitrogen migrated from the feedstock to the biocrude, a slight increase of N in the biocrude for Bag:Chl and Bag:Cy of 6% and 3%, respectively. This could be attributed to the Maillard reaction between amino acids from protein hydrolysis of algae and reducing sugar from the hydrolysis of the carbohydrates of bagasse, which leads to the production of N-containing compounds in the biocrude [65].

Carbon from algae HTL was mostly retained in the biocrude fraction in the range of 50–67% for *Cyanobacteria* and 35–56% for *Chlorella vulgaris*. In comparison for bagasse, carbon is in the solid residue product (40–50%), the increase of temperature leads to the recovery of more carbon in the biocrude. In the co-liquefaction of bagasse: algae mixture at 250 °C, 45% of carbon was recovered mostly in the solid residue. However, increasing of temperature led to the migration of carbon to the biocrude and the aqueous phase. Carbon recovered in the gaseous phase (mainly as CO_2) was in the range of 5–11%. Similarly, Guo et al. [18], recovered CO_2 in the gaseous phase in the range of 0–8.7% at 200–280 °C, further demonstrating that higher temperatures result in higher carbon recovered in the gaseous phase.

Sulphur was mainly retained in the aqueous phase (60–80%) in this study. The sulphur recovered in the aqueous phase explains its low pH of 3–4.5. Sulphur exists as water-soluble compounds such as benzothiazole, which was identified in the aqueous phase of HTL biocrude from yeast [66]. Increase temperatures led to the retention of more sulphur in the biocrude. Less sulphur was retained in the biocrude from the co-liquefaction of Bag: *Cy* of 20% compared to 34% recovered in the *Cyanobacteria* biocrude.

Bagasse biocrude is mainly composed of alcohols, aromatics and cyclic oxygenates and ketones [67] and algae biocrude is generally composed of hydrocarbons, polyaromatic N-compounds, straight and

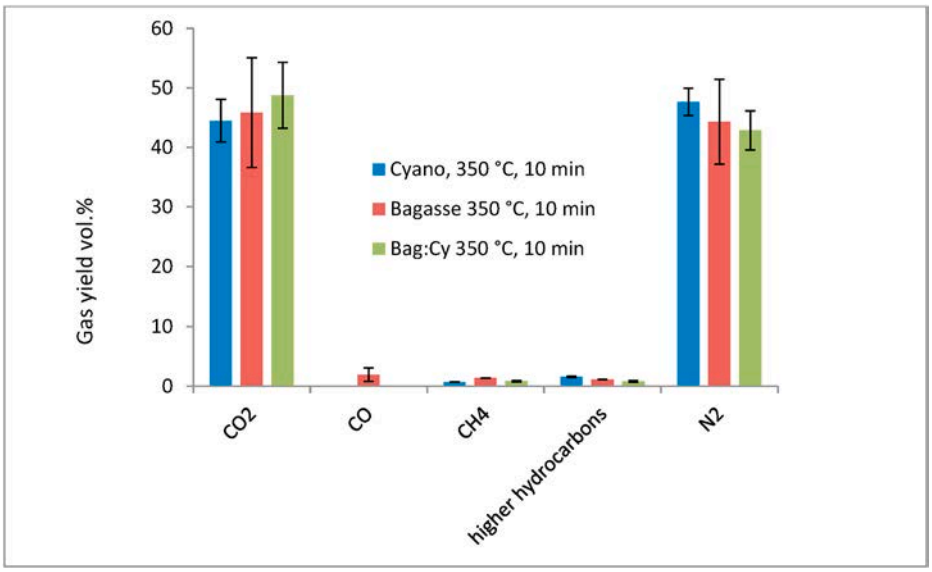

Fig. 12. Compounds identified in the gaseous products from hydrothermal liquefaction at 350 °C.

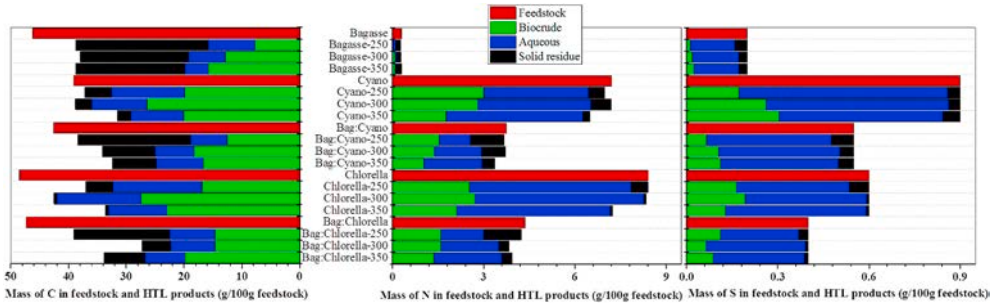

Fig. 13. C, N and S distribution in the HTL products at 250, 300 and 350 °C.

branched amides [10].

4. Conclusions

The highest HTL biocrude yield of the different algae species was attained at different conditions. For *Cyanobacteria*, the highest biocrude yield of 47.57 wt% was attained at 300 °C, 60 min, while that for *Chlorella vulgaris* (43 wt%) at 350 °C, 10 min. N content was reduced in the biocrude by the increasing temperature, whereas residence time did not have a significant influence. Multi-criterion analysis showed that biocrude yield is correlated with lipids and proteins fractions and the carbon content of the algae species. Carbohydrates fraction is anti-correlated to biocrude yield. In conclusion, PCA is a powerful tool to investigate the correlation between biochemical composition of feedstock, HTL conditions (i.e. T and RT) on HTL products yields and biocrude properties.

Co-liquefaction of algae (*Cyanobacteria* and *Chlorella vulgaris*) with lignocellulosic biomass (bagasse) showed an improved biocrude yield. The maximum biocrude yield of 54 wt% at 350 °C, 10 min was for bagasse and *Cyanobacteria* mixture (1:1) while 43% was obtained for bagasse and *Chlorella vulgaris* mixture (1:1) at 300 °C, 60 min. N and S contents of the Cyanobacteria biocrude, 7% and 0.7% were reduced to 4.6% and 0.3% respectively for Bagasse: Cyanobacteria biocrude, yet with slightly higher oxygen (O). Thus it is expected that concentrations of amides and N-heterocyclic compounds to be reduced with a possible increase in O-heterocyclic compounds.

Acknowledgement

The authors appreciatively acknowledge the financial support provided by QUT, a PhD scholarship from the School of Chemistry, Physics and Mechanical Engineering and an ECARD grant. The authors would like to extend their thanks to Armin Lautenbach, Birgit Rolli, Alexandra Bohm, Jessica Mayer, and Sonja Habicht for their technical assistance and Thomas Tietz and Matthias Pagel for the mechanical support at Karlsruhe Institute of Technology.

References

[1] Central Intelligence Agency, The world factbook. https://www.cia.gov/library/publications/the-world-factbook/index.html, 2016.
[2] C.A.S. Hall, J.G. Lambert, S.B. Balogh, EROI of different fuels and the implications for society, Energy Pol. 64 (2014) 141–152, https://doi.org/10.1016/j.enpol.2013.05.049.
[3] L. Wagner, I. Ross, J. Foster, B. Hankamer, Trading off global fuel supply, CO2 emissions and sustainable development, PloS One 11 (2016) 1–17.
[4] International Energy Agency, 2017 world energy outlook, n.d, https://www.iea.org/weo2017, 2017.
[5] United Nations, Adoption of the Paris Agreement, vol. 8, 2015.
[6] K. Araújo, D. Mahajan, R. Kerr, M da Silva, Global biofuels at the crossroads: an overview of technical, policy, and investment complexities in the sustainability of biofuel development, Agriculture 7 (2017) 32.
[7] United Nations, n.d), https://sustainabledevelopment.un.org/?menu 1300.
[8] O.M. Adeniyi, U. Azimov, A. Burluka, Algae biofuel: current status and future applications, Renew. Sustain. Energy Rev. 90 (2018) 316–335.
[9] A.J. Ward, D.M. Lewis, F.B. Green, Anaerobic digestion of algae biomass: a review, Algal Res 5 (2014) 204–214.
[10] Y. Guo, T. Yeh, W. Song, D. Xu, S. Wang, A review of bio-oil production from hydrothermal liquefaction of algae, Renew. Sustain. Energy Rev. 48 (2015) 776–790.
[11] J.A. Ramirez, R.J. Brown, T.J. Rainey, A review of hydrothermal liquefaction bio-crude properties and prospects for upgrading to transportation fuels, Energies 8 (2015) 6765–6794.
[12] D. Xu, G. Lin, S. Guo, S. Wang, Y. Guo, Z. Jing, Catalytic hydrothermal liquefaction of algae and upgrading of biocrude: a critical review, Renew. Sustain. Energy Rev. 97 (2018) 103–118.
[13] D. López Barreiro, B.R. Gómez, F. Ronsse, U. Hornung, A. Kruse, W. Prins, Heterogeneous catalytic upgrading of biocrude oil produced by hydrothermal liquefaction of microalgae: state of the art and own experiments, Fuel Process. Technol. 148 (2016) 117–127.
[14] G.H.C. Prado, Y. Rao, A. De Klerk, Nitrogen removal from oil: a review, Energy Fuels 31 (2017) 14–36.
[15] J. Yu, K. Maliutina, A. Tahmasebi, A review on the production of nitrogen-containing compounds from microalgal biomass via pyrolysis, Bioresour. Technol. 270 (2018) 689–701.
[16] S.O. Lourenço, E. Barbarino, P.L. Lavín, U.M. Lanfer Marquez, E. Aidar, Distribution of intracellular nitrogen in marine microalgae: calculation of new nitrogen-to-protein conversion factors, Eur. J. Phycol. 39 (2004) 17–32, https://doi.org/10.1080/0967026032000157156.
[17] Y. Dote, S. Inoue, T. Ogi, S.Y. Yokoyama, Distribution of nitrogen to oil products from liquefaction of amino acids, Bioresour. Technol. 64 (1998) 157–160.
[18] G. Yu, Y. Zhang, L. Schideman, T. Funk, Z. Wang, Distributions of carbon and nitrogen in the products from hydrothermal liquefaction of low-lipid microalgae, Energy Environ. Sci. 4 (2011) 4587–4595.
[19] C.K. Shu, Pyrazine formation from amino acids and reducing sugars, a pathway other than strecker degradation, J. Agric. Food Chem. 46 (1998) 1515–1517.
[20] W. Yang, X. Li, Z. Li, C. Tong, L. Feng, Understanding low-lipid algae hydrothermal liquefaction characteristics and pathways through hydrothermal liquefaction of algal major components: crude polysaccharides, crude proteins and their binary mixtures, Bioresour. Technol. 196 (2015) 99–108.
[21] J. Yang, , He Q (Sophia), H. Niu, K. Corscadden, T. Astatkie, Hydrothermal liquefaction of biomass model components for product yield prediction and reaction pathways exploration, Appl. Energy 228 (2018) 1618–1628.
[22] Y. Fan, U. Hornung, N. Dahmen, A. Kruse, Hydrothermal liquefaction of protein-containing biomass: study of model compounds for Maillard reactions, Biomass Convers Biorefinery 8 (2018) 909–923.
[23] J. Yang, , He Q (Sophia), H. Niu, K. Corscadden, T. Astatkie, Hydrothermal liquefaction of biomass model components for product yield prediction and reaction pathways exploration, Appl. Energy 228 (2018) 1618–1628.
[24] A. Sinag, A. Kruse, P. Maniam, Hydrothermal conversion of biomass and different model compounds, J. Supercrit. Fluids 71 (2012) 80–85, https://doi.org/10.1016/j.supflu.2012.07.010.
[25] L. Sheng, X. Wang, X. Yang, Prediction model of biocrude yield and nitrogen heterocyclic compounds analysis by hydrothermal liquefaction of microalgae with model compounds, Bioresour. Technol. 247 (2018) 14–20, https://doi.org/10.1016/j.biortech.2017.08.011.
[26] C. Gai, Y. Li, N. Peng, A. Fan, Z. Liu, Co-liquefaction of microalgae and lignocellulosic biomass in subcritical water, Bioresour. Technol. 185 (2015) 240–245.
[27] W.T. Chen, Y. Zhang, J. Zhang, L. Schideman, G. Yu, P. Zhang, et al., Co-liquefaction of swine manure and mixed-culture algal biomass from a wastewater treatment system to produce bio-crude oil, Appl. Energy 128 (2014) 209–216.
[28] D.W.F. Brilman, N. Drabik, M. Wądrzyk, Hydrothermal co-liquefaction of microalgae, wood, and sugar beet pulp, Biomass Convers Biorefinery 7 (2017) 445–454.
[29] Y. Hu, S. Feng, A. Bassi, C. Xu, Charles), Improvement in bio-crude yield and quality through co-liquefaction of algal biomass and sawdust in ethanol-water

mixed solvent and recycling of the aqueous by-product as a reaction medium, Energy Convers. Manag. 171 (2018) 618–625.
[30] D. Castello, T.H. Pedersen, Continuous Hydrothermal Liquefaction of Biomass : A Critical Review, 2018, https://doi.org/10.3390/en11113165.
[31] A. Friedl, E. Padouvas, H. Rotter, K. Varmuza, Prediction of heating values of biomass fuel from elemental composition, Anal. Chim. Acta 544 (2005) 191–198.
[32] R.B. Madsen, R.Z.K. Bernberg, P. Biller, J. Becker, B.B. Iversen, M. Glasius, Hydrothermal co-liquefaction of biomasses-quantitative analysis of bio-crude and aqueous phase composition, Sustain Energy Fuels 1 (2017) 789–805.
[33] N.C. Surawski, B. Miljevic, T.A. Bodisco, R.J. Brown, Z.D. Ristovski, G.A. Ayoko, Application of multicriteria decision making methods to compression ignition engine efficiency and gaseous, particulate, and greenhouse gas emissions, Environ. Sci. Technol. 47 (2013) 1904–1912.
[34] Surawski N, Van TC, Ristovski Z, Cong NL, Lan HN, Yuan C-SJ, et al. Effects of Sulphur and Vanadium Contents in Diesel Fuel on Engine Performance and Emissions: Principal Component Analysis (PCA). 11th Asia-Pacific Conf Combust ASPACC 2017 2017;2017-Decem.
[35] F. Husson, Multivariate Exploratory Data Analysis and Data Mining, 2017.
[36] W. Revelle, Procedures for Psychological, Psychometric and Personality Research, 2017.
[37] R. Wehrens, in: R. Gentleman, K. Hornik, G. Parmigiani (Eds.), Chemometrics with R. Multivariate Data Analysis in the Natural Sciences and Life Sciences, 2011.
[38] G.A. Ayoko, L. Morawska, S. Kokot, D. Gilbert, Application of multicriteria decision making methods to air quality in the microenvironments of residential houses in brisbane, Australia, Environ. Sci. Technol. 38 (2004) 2609–2616.
[39] B. Espinasse, G. Picolet, E. Chouraqui, Negotiation support systems: a multi-criteria and multi-agent approach, Eur. J. Oper. Res. 103 (1997) 389–409.
[40] M.A. Islam, R.J. Brown, P.R. Brooks, M.I. Jahirul, H. Bockhorn, K. Heimann, Investigation of the effects of the fatty acid profile on fuel properties using a multi-criteria decision analysis, Energy Convers. Manag. 98 (2015) 340–347.
[41] A. Campanella, R. Muncrief, M.P. Harold, D.C. Griffith, N.M. Whitton, R.S. Weber, Thermolysis of microalgae and duckweed in a CO2-swept fixed-bed reactor: bio-oil yield and compositional effects, Bioresour. Technol. 109 (2012) 154–162.
[42] I.V. Babich, M. van der Hulst, L. Lefferts, J.A. Moulijn, P. O'Connor, K. Seshan, Catalytic pyrolysis of microalgae to high-quality liquid bio-fuels, Biomass Bioenergy 35 (2011) 3199–3207.
[43] H.H. Bui, K.Q. Tran, W.H. Chen, Pyrolysis of microalgae residues - a kinetic study, Bioresour. Technol. 199 (2015) 362–366.
[44] N. Muradov, B. Fidalgo, A.C. Gujar, A. T-Raissi, Pyrolysis of fast-growing aquatic biomass - lemna minor (duckweed): characterization of pyrolysis products, Bioresour. Technol. 101 (2010) 8424–8428.
[45] X. Wang, L. Sheng, X. Yang, Pyrolysis characteristics and pathways of protein, lipid and carbohydrate isolated from microalgae Nannochloropsis sp, Bioresour. Technol. 229 (2017) 119–125.
[46] D. Lopez Barreiro, C. Zamalloa, N. Boon, W. Vyverman, F. Ronsse, W. Brilman, et al., Influence of strain-specific parameters on hydrothermal liquefaction of microalgae, Bioresour. Technol. 146 (2013) 463–471.
[47] P. Duan, Z. Chang, Y. Xu, X. Bai, F. Wang, L. Zhang, Hydrothermal processing of duckweed: effect of reaction conditions on product distribution and composition, Bioresour. Technol. 135 (2013) 710–719.
[48] Y. Dote, S. Sawayama, S. Inoue, T. Minowa, S ya Yokoyama, Recovery of liquid fuel from hydrocarbon-rich microalgae by thermochemical liquefaction, Fuel 73 (1994) 1855–1857.
[49] P. Duan, B. Jin, Y. Xu, Y. Yang, X. Bai, F. Wang, et al., Thermo-chemical conversion of Chlorella pyrenoidosa to liquid biofuels, Bioresour. Technol. 133 (2013) 197–205.
[50] U. Jena, K.C. Das, J.R. Kastner, Effect of operating conditions of thermochemical liquefaction on biocrude production from Spirulina platensis, Bioresour. Technol. 102 (2011) 6221–6229.
[51] P. Biller, A.B. Ross, Potential yields and properties of oil from the hydrothermal liquefaction of microalgae with different biochemical content, Bioresour. Technol. 102 (2011) 215–225.
[52] M.E. Ross, K. Davis, R. McColl, M.S. Stanley, J.G. Day, A.J.C. Semiao, Nitrogen uptake by the macro-algae Cladophora coelothrix and Cladophora parriaudii: influence on growth, nitrogen preference and biochemical composition, Algal Res 30 (2018) 1–10.
[53] M.A. Islam, M. Magnusson, R.J. Brown, G.A. Ayoko, M.N. Nabi, K. Heimann, Microalgal species selection for biodiesel production based on fuel properties derived from fatty acid profiles, Energies 6 (2013) 5676–5702.
[54] H. Li, Z. Liu, Y. Zhang, B. Li, H. Lu, N. Duan, et al., Conversion efficiency and oil quality of low-lipid high-protein and high-lipid low-protein microalgae via hydrothermal liquefaction, Bioresour. Technol. 154 (2014) 322–329.
[55] N. Sato, A.T. Quitain, K. Kang, H. Daimon, K. Fujie, Reaction kinetics of amino acid decomposition in high-temperature and high-pressure water, Ind. Eng. Chem. Res. 43 (2004) 3217–3222.
[56] Y. Huang, Y. Chen, J. Xie, H. Liu, X. Yin, C. Wu, Bio-oil production from hydrothermal liquefaction of high-protein high-ash microalgae including wild Cyanobacteria sp. and cultivated Bacillariophyta sp, Fuel 183 (2016) 9–19.
[57] S.S. Toor, H. Reddy, S. Deng, J. Hoffmann, D. Spangsmark, L.B. Madsen, et al., Hydrothermal liquefaction of Spirulina and Nannochloropsis salina under subcritical and supercritical water conditions, Bioresour. Technol. 131 (2013) 413–419.
[58] D. Zhou, L. Zhang, S. Zhang, H. Fu, J. Chen, Hydrothermal liquefaction of macroalgae enteromorpha prolifera to bio-oil, Energy Fuels 24 (2010) 4054–4061.
[59] D. Xu, G. Lin, L. Liu, Y. Wang, Z. Jing, S. Wang, Comprehensive evaluation on product characteristics of fast hydrothermal liquefaction of sewage sludge at different temperatures, Energy 159 (2018) 686–695.
[60] D. Xu, P.E. Savage, Effect of temperature, water loading, and Ru/C catalyst on water-insoluble and water-soluble biocrude fractions from hydrothermal liquefaction of algae, Bioresour. Technol. 239 (2017) 1–6.
[61] G. Teri, L. Luo, P.E. Savage, Hydrothermal treatment of protein, polysaccharide, and lipids alone and in mixtures, Energy Fuels 28 (2014) 7501–7509.
[62] Brilman DWF (Wim) C. Torri, L. Garcia Alba, C. Samorì, D. Fabbri, Hydrothermal treatment (HTT) of microalgae: detailed molecular characterization of HTT oil in view of HTT mechanism elucidation, Energy Fuels 26 (2012) 658–671.
[63] Australian Government Department of Environment and Energy, Diesel fuel quality standard. https://www.environment.gov.au/protection/fuel-quality/standards/diesel, 2001.
[65] A.A. Peterson, F. Vogel, R.P. Lachance, M. Froling, M.J. Antal, J.W. Tester, Thermochemical biofuel production in hydrothermal media: a review of sub- and supercritical water technologies, Energy Environ. Sci. 1 (2008) 32–65.
[66] Z. Bi, J. Zhang, Z. Zhu, Y. Liang, T. Wiltowski, Generating biocrude from partially defatted Cryptococcus curvatus yeast residues through catalytic hydrothermal liquefaction, Appl. Energy 209 (2018) 435–444.
[67] J. Kosinkova, J.A. Ramirez, J. Nguyen, Z. Ristovski, R. Brown, C.S.K. Lin, et al., Hydrothermal liquefaction of bagasse using ethanol and black liquor as solvents, Biofuels, Bioprod Biorefining 6 (2015) 246–256.